Data-adaptive Robust Optimization Method for the Economic Dispatch of Active Distribution Networks

Zhang, Yipu; Ai , Xiaomeng; Fang, Jiakun; Wen, Jinyu; He, Haibo

Published in:
I E E E Transactions on Smart Grid

DOI (link to publication from Publisher):
10.1109/TSG.2018.2834952

Publication date:
2019

Document Version
Accepted author manuscript, peer reviewed version

This article has been accepted for publication in a future issue of this journal, but has not been fully edited. Content may change prior to final publication. Citation information: DOI 10.1109/TSG.2018.2834952, IEEE Transactions on Smart Grid

Data-adaptive Robust Optimization Method for the Economic Dispatch of Active Distribution Networks

Yipu Zhang, *Student Member, IEEE,* Xiaomeng Ai, *Member, IEEE,* Jiakun Fang, *Member, IEEE,* Jinyu Wen, *Member, IEEE,* and Haibo He, *Fellow, IEEE*

***Abstract*—Due to the restricted mathematical description of the uncertainty set, the current two-stage robust optimization is usually over-conservative which has drawn concerns from the power system operators. This paper proposes a novel data-adaptive robust optimization method for the economic dispatch of active distribution network with renewables. The scenario-generation method and the two-stage robust optimization are combined in the proposed method. To reduce the conservativeness, a few extreme scenarios selected from the historical data are used to replace the conventional uncertainty set. The proposed extreme-scenario selection algorithm takes advantage of considering the correlations and can be adaptive to different historical data sets. A theoretical proof is given that the constraints will be satisfied under all the possible scenarios if they hold in the selected extreme scenarios, which guarantees the robustness of the decision. Numerical results demonstrate that the proposed data-adaptive robust optimization algorithm with the selected uncertainty set is less conservative but equally as robust as the existing two-stage robust optimization approaches. This leads to the improved economy of the decision with uncompromised security.**

***Index Terms*—Distributed renewable generation, economic dispatch, active distribution networks, data-adaptive robust optimization, extreme scenario**

NOMENCLATURE OF THE ECONOMIC DISPATCH

Parameters

E/B	Set of branches/buses
r_{ij}/x_{ij}	Resistor and reactance of branch (i, j)
$\delta(j)$	Set of the child nodes of bus j
$\pi(j)$	Set of the parent nodes of bus j
$I_{ij,max}$	Maximum current of the branch (i, j)
$U_{j,min}/U_{j,max}$	Lower/upper bound voltage of bus j
$Q_{c,j,min}/Q_{c,j,max}$	Lower/upper bound of reactive power injection of the SVG at bus j
$P_{L,j}/Q_{L,j}$	Active/reactive power of the load at bus j
s_j	Admittance of each switching capacitor bank at bus j
$C_{j,min}/C_{j,max}$	Min/max capacitance of the switching capacitors at bus j
n_{ij}	Number of the transformer taps of branch (i, j)

Variables

I_{ij}	Current flowing through branch (i, j)
U_j	Voltage of bus j
P_{ij}/Q_{ij}	Active/reactive power flow from bus i to bus j
$P_{G,j}/Q_{G,j}$	Active/reactive power of the connection point between the transmission network and the distribution network
$P_{DG,j}$	Active power of the distributed generation at bus j
$Q_{c,j}$	Reactive power of the SVG at bus j
C_j	Admittance of the switching capacitors at bus j
b_j	Number of the switching capacitor banks in operation at bus j
t_{ij}	Tap ratio of the transformer branch (i, j) and assuming the possible value to be $t_{ij,1}, t_{ij,2}$ ...

I. INTRODUCTION

In recent years, policy inventiveness and public awareness on the fossil-fuel depletion promote rapid development and increased deployment of renewable power generations [1][2], especially distributed renewable generations (DRGs). Take China for example, according to the National Energy Administration, the total installed capacity of distributed power will reach 187 GW by 2020, accounting for 9.1% of the national total generation capacity [3][4]. With the increasing penetration of the DRGs, the traditional distribution networks will be

This work was supported in part by the National Nature Science Foundation of China (51707070), and in part by the National Key Research and Development Program of China (2016YFB0900400, 2016YFB0900403).

Y. Zhang, X. Ai (corresponding author), and J. Wen are with State Key Laboratory of Advanced Electromagnetic Engineering and Technology, School of Electrical and Electronic Engineering, Huazhong University of Science and Technology, Wuhan 430074, China (e-mail: zypsc@hust.edu.cn; xiaomengai1986@foxmail.com; jinyu.wen@hust.edu.cn)

J. Fang is with the Department of Energy Technology, Aalborg University, Aalborg DK-9220, Denmark (e-mail: jiakun.fang@gmail.com)

H. He is with the Department of Electrical, Computer and Biomedical Engineering, University of Rhode Island, Kingston, RI 02881 USA (e-mail: he@ele.uri.edu)

gradually transformed into the active distribution networks (ADNs). However, the uncertainties of the renewables challenge the system operation [5]-[10].

To encounter the uncertainties brought by the DRGs, various methods and optimization models have been proposed with different stochastic variables and constraints embedded, e.g. probabilistic load flow [11]-[13], scenario-based optimization [14]-[18], chance-constrained optimization [19]-[21], and robust optimization [22]-[33], to name a few. The two-stage stochastic programming is proposed in [15] and [16], and the uncertainties are described using a set of scenarios. Furthermore, the decomposition algorithms are also employed to reduce the computational burden. In [19], a chance-constrained two-stage stochastic program is proposed, and the sample average approximation algorithm is employed to solve this two-stage model effectively. Compared with the chance-constrained optimization and the scenario-based optimization, robust optimization has the following advantages: 1) limited and easy-to-obtain empirical or predictive knowledge is required; 2) the computational burden is alleviated using a robust counterpart instead of huge numbers of scenarios; 3) robust optimization models are usually easy to understand and implement.

However, robust optimization methods also have two major drawbacks: 1) if the model is nonlinear or non-convex, the robust counterpart could be intractable, and the decomposition algorithm, such as the Benders' decomposition algorithm and column-and-constraints generation (C&CG) algorithm, might be invalid; 2) the optimal solution might be too conservative and, sometimes, being robust to unnecessary situations could even result in infeasibilities.

Hence, the robust optimization was difficult to apply to the economic dispatch of ADNs before the work in [34] and [35], because the economic dispatch of the distribution system was usually formulated as a non-convex AC optimal power flow (ACOPF) problem [36] [37]. In [34], the phase angle relaxation and conic relaxation are employed to reformulate the ACOPF model to second-order cone programming (SOCP). With this convexity, the two-stage robust reactive power optimization in active distribution networks is proposed and then effectively solved by the C&CG algorithm in [29]-[31].

Though the intractability of the robust optimization due to the non-convexity is solved, the second problem of robust optimization remains because of the crude description of uncertainties [27]. Traditionally, the cubic set is defined as the robust region [28]-[32]. With growing operational experience and the advancement of the data-driven techniques, adopting data-processing techniques in robust optimization is promising [38]-[44]. In [27], the minimum volume enclosing ellipsoid (MVEE) algorithm is proposed to identify the uncertainty set of the output of renewables for robust optimization, and the conservativeness of the solution is reduced compared to the traditional robust optimization with cubic robust regions [33]. But using the ellipsoidal uncertainty sets will change the mathematical property of the model. For example, the model of the security constrained economic dispatch (SCED) in [33] is transformed from the linear programming to the SOCP after the robust transformation using the ellipsoidal uncertainty set. If the original problem is not linear, such as the economic dispatch of the distribution system, the MVEE algorithm may lead to a higher-order optimization problem.

This paper proposes a data-adaptive robust optimization (DARO) method for the economic dispatch of ADNs. The proposed method bridges the recent advances in scenario generation and the robust optimization techniques. The algorithmic and practical contributions of this work include:

(1) The novel data-adaptive set is proposed to describe the uncertainty of stochastic variables which helps to improve the economy while maintaining the robustness of the decision.

(2) Few extreme scenarios are selected from the historical records of the stochastic variables to consist the robust region. Besides, the number of extreme scenarios will not increase exponentially with the number of the stochastic variables, which helps to alleviate the computational burden.

(3) The property of the original problem is the same as the transformed model so that the tractability of the transformed optimization is ensured once the original model is linear or convex.

(4) The proposed DARO method can be easily expanded to the other convex programming in power systems.

The rest of the paper is organized as follows: Section II presents the general mathematical formulation for the economic dispatch of ADNs. In Section III, the DARO method is proposed. In Section IV, numeric results on a 33-bus system and a 123-bus system are shown to illustrate the effectiveness of the proposed model. Finally, conclusions are drawn in Section V.

II. Problem Formulation

A. Description of the economic dispatch

This economic dispatch of ADNs based on the branch flow model [34] with minimum active power loss as the objective function can be formulated as:

$$\min \sum r_{ij} \cdot I_{ij}^2 \quad \forall (i,j) \in E \tag{1}$$

Subject to following constraints:

$$P_{ij}^2 + Q_{ij}^2 = I_{ij}^2 U_i^2 \quad \forall (i,j) \in E \tag{2}$$

$$U_j^2 t_{ij}^{-2} = U_i^2 + (r_{ij}^2 + x_{ij}^2) I_{ij}^2 - 2(r_{ij} P_{ij} + x_{ij} Q_{ij}) \ \forall (i,j) \in E \tag{3}$$

$$Q_{G,j} + U_j^2 C_j + Q_{c,j} - Q_{L,j} = \sum_{k \in \delta(j)} Q_{jk} - \sum_{i \in \pi(j)} (Q_{ij} - x_{ij} I_{ij}^2) \ \forall j \in B \tag{4}$$

$$P_{G,j} + P_{DG,j} - P_{L,j} = \sum_{k \in \delta(j)} P_{jk} - \sum_{i \in \pi(j)} (P_{ij} - r_{ij} I_{ij}^2) \ \forall j \in B \tag{5}$$

$$I_{ij} \le I_{ij,\max} \quad \forall (i,j) \in E \tag{6}$$

$$U_{j,\max} \le U_j \le U_{j,\min} \quad \forall j \in B \tag{7}$$

$$t_{ij} \in \left\{ t_{ij,1}, t_{ij,2} \ldots t_{ij,n_{ij}} \right\} \forall (i,j) \in E \tag{8}$$

$$C_{j,\min} \le C_j = b_j s_j \le C_{j,\max} \tag{9}$$

$$Q_{cj,\min} \le Q_{c,j} \le Q_{cj,\max} \ \forall j \in B \tag{10}$$

Constraints (2)–(5) are the nodal power balance and branch

flow equations in the ADNs, where $P_{DG,j}$ are stochastic. Constraints (6)–(7) are the upper and lower bounds of the current and voltage magnitude for each branch and bus. Besides, constraints (8)–(10) are the operational limits for the reactive power compensation devices. The transformer taps t_{ij}, and the switching capacitor banks C_j are discrete variables, which should be decided one day before and cannot be changed in daily operation. To deal with the optimization (1)–(10) effectively, the method in [30] and [45] are employed to convexify the original model. First, dummy variables l_{ij} and u_j are introduced to replace the square terms I_{ij}^2 and U_j^2, respectively. Furthermore, (1)–(7) can be rewritten as:

$$\min \sum r_{ij} \cdot l_{ij} \quad \forall (i,j) \in E \tag{11}$$

$$P_{ij}^2 + Q_{ij}^2 = l_{ij} u_i \ \forall (i,j) \in E \tag{12}$$

$$u_j t_{ij}^{-2} = u_i + (r_{ij}^2 + x_{ij}^2) l_{ij} - 2(r_{ij} P_{ij} + x_{ij} Q_{ij}) \ \forall (i,j) \in E \tag{13}$$

$$Q_{G,j} + u_j b_j s_j + Q_{c,j} - Q_{L,j} = \sum_{k \in \delta(j)} Q_{jk} - \sum_{i \in \pi(j)} (Q_{ij} - x_{ij} l_{ij}) \ \forall j \in B \tag{14}$$

$$P_{G,j} + P_{DG,j} - P_{L,j} = \sum_{k \in \delta(j)} P_{jk} - \sum_{i \in \pi(j)} (P_{ij} - r_{ij} l_{ij}) \ \forall j \in B \tag{15}$$

$$l_{ij} \le I_{ij,\max}^2 \ \forall (i,j) \in E \tag{16}$$

$$U_{j,\min}^2 \le u_j \le U_{j,\max}^2 \quad \forall j \in B \tag{17}$$

The nonlinear terms generated by (13) can be exactly linearized using the big M approach [45]:

$$\begin{cases} t_{ij}^{-2} = r_{ij,1} \cdot t_{ij,1}^{-2} + \ldots + r_{ij,n_{ij}} \cdot t_{ij,n_{ij}}^{-2} \\ u_j t_{ij}^{-2} = h_{j,1} \cdot t_{ij,1}^{-2} + \ldots + h_{j,n_{ij}} \cdot t_{ij,n_{ij}}^{-2} \end{cases} \tag{18}$$

$$\sum_{k=1}^{n_{ij}} r_{ij,k} = 1 \ \ r_{ij,k} \in \{0,1\} \quad \forall (i,j) \in E \tag{19}$$

$$\begin{cases} -M r_{ij,k} \le h_{j,k} \le M r_{ij,k} \\ -M(1 - r_{ij,k}) + u_j \le h_{j,k} \le M(1 - r_{ij,k}) + u_j \end{cases} \tag{20}$$

where $h_{j,k}$ is a dummy variable and $r_{ij,k}$ is binary. M is a sufficiently large number. Substituting the left-hand side in (13):

$$\sum_{k=1}^{n_{ij}} h_{j,k} \cdot t_{ij,k}^{-2} = u_i + (r_{ij}^2 + x_{ij}^2) l_{ij} - 2(r_{ij} P_{ij} + x_{ij} Q_{ij}) \tag{21}$$

As for the nonlinear terms $u_j b_j$ in (14), they can be linearized by replacing the discrete number b_j with a combination of series of binary variables θ_{j,v_j}:

$$\begin{cases} b_j = 2^0 \theta_{j,1} + \cdots + 2^{v_j - 1} \theta_{j,v_j} \\ u_j b_j = 2^0 \sigma_{j,1} + \cdots + 2^{v_j - 1} \sigma_{j,v_j} \end{cases} \tag{22}$$

Then the big M approach is used in the same way as the previous step:

$$\begin{cases} -M \theta_{j,k} \le \sigma_{j,k} \le M \theta_{j,k} \\ -M(1 - \theta_{j,k}) + u_j \le \sigma_{j,k} \le M(1 - \theta_{j,k}) + u_j \end{cases} \tag{23}$$

where $\sigma_{j,k}$ is a dummy variable, and $\theta_{j,k}$ is binary. Integer v_j denotes the bit of the binary and can be determined by (24):

$$v_j = \begin{cases} \left[\log_2 \left(C_{j,\max} / s_j \right) \right] + 1 & C_{j,\max} \ne 0 \\ 1 & C_{j,\max} = 0 \end{cases} \tag{24}$$

where the operation $[\bullet]$ denotes rounding to zero. Constraints (9) and (14) can be reformulated correspondingly as:

$$C_{j,\min} \le s_j \cdot \sum_{k=1}^{v_j} \left(2^{k-1} \cdot \theta_{j,k} \right) \le C_{j,\max} \quad \theta_{j,k} \in \{0,1\} \tag{25}$$

$$Q_{G,j} + s_j \sum_{k=1}^{v_j} 2^{k-1} \sigma_{j,k} + Q_{c,j} - Q_{L,j} = \sum_{k \in \delta(j)} Q_{jk} - \sum_{i \in \pi(j)} \left(Q_{ij} - x_{ij} l_{ij} \right) \forall j \in B \tag{26}$$

As for constraint (12), it can be re-formulated as (27) using the second order cone relaxation [34][35]:

$$P_{ij}^2 + Q_{ij}^2 \le l_{ij} u_i \ \forall (i,j) \in E \tag{27}$$

Finally, the original model (1)-(10) are convexified. The objective function of the original model can be reformulated as (11). The constraints are replaced with (10), (15)-(17), (19)-(21), (23), (25)-(27). Its compact form can be written as:

$$\begin{aligned} &\min \ \ q(\boldsymbol{\omega}, \boldsymbol{x}, \boldsymbol{y}) \\ &s.t \ \ f(\boldsymbol{\omega}, \boldsymbol{x}, \boldsymbol{y}) = 0 \ \ g(\boldsymbol{\omega}, \boldsymbol{x}, \boldsymbol{y}) \le 0 \end{aligned} \tag{28}$$

where q is the objective function denoted by (11). Here, f denotes the equality constraints (15), (19), (21), (26); g denotes the inequality constraints (10), (16), (17), (20), (23), (25), (27); and $\boldsymbol{\omega}$ is a stochastic vector denoting the values of $P_{DG,j}$ and is always defined using the uncertainty set in the robust optimizations. $\boldsymbol{x}$ denotes the decision variables associated with the flexible facilities, such as the reactive power of the SVG and the power exchange with the upper-level grid. Their values can be changed at any time if the DRG generations deviate from the forecast. $\boldsymbol{y}$ denotes the decision variables associated with the inflexible facilities, such as the tap ratio of the transformers and the statuses of the switching capacitors banks. Once these variables are determined in advance, they cannot be changed for several hours in the future.

B. Conservativeness of the current two-stage robust optimization

The two-stage robust optimization (TRO) is adopted here to model optimization problems with uncertainties. At the first stage, a "here-and-now" decision $\boldsymbol{y}$ should be made before the instance of the uncertain data $\boldsymbol{\omega}$ is given. The decision $\boldsymbol{y}$ should be robust to all of the instances defined in the uncertainty set. At the second stage, once an instance of $\boldsymbol{\omega}$ is derived, the flexible variable $\boldsymbol{x}$ can be obtained by solving a corresponding optimization problem with the given $\boldsymbol{y}$. It can be seen that the uncertainty set influences the decisions directly. Generally, the uncertainty set can be mathematically described as either a cubic set or an ellipsoid as shown in (29) and (30), respectively.

$$\boldsymbol{\omega} \in W_1 = \left\{ \boldsymbol{\omega} \in \boldsymbol{R}^n \left| \boldsymbol{\omega}_{\min} \le \boldsymbol{\omega} \le \boldsymbol{\omega}_{\max} \right. \right\} \tag{29}$$

$$\boldsymbol{\omega} \in W_2 = \{ \boldsymbol{\omega} \in \boldsymbol{R}^n \left| (\boldsymbol{\omega} - \boldsymbol{c})^T Q (\boldsymbol{\omega} - \boldsymbol{c}) \le 1 \right. \} \tag{30}$$

This article has been accepted for publication in a future issue of this journal, but has not been fully edited. Content may change prior to final publication. Citation information: DOI 10.1109/TSG.2018.2834952, IEEE Transactions on Smart Grid

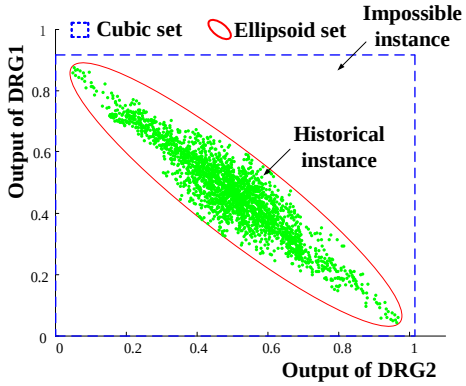

Fig. 1. The cubic set and the ellipsoid set

But in practice, the cubic set fails to take the correlations of multiple DRGs into account. It can be seen from Fig. 1 that the cubic set covers too large of an area, containing a lot of impossible instances for the output of DRGs that the decision has no need to be robust to. Meanwhile, if the ellipsoid is used, the mathematical property of the optimization could be changed, because the ellipsoid usually has a second-order formula. To overcome these two disadvantages, the DARO method is proposed in the next section.

III. The Two-Stage DARO Method

The DARO proposed method considers the correlations of the DRGs by building a data-adaptive set shown as (31).

$$\boldsymbol{\omega} \in W_3 = \left\{ \boldsymbol{\omega} \in \boldsymbol{R}^n \left| \begin{array}{l} \boldsymbol{\omega} = \sum_{i=1}^{N_e} p_i \boldsymbol{\omega}_{e,i} \\ \sum_{i=1}^{N_e} p_i = 1,\ p_i \geq 0 \end{array} \right. \right\} \tag{31}$$

where $\boldsymbol{\omega}_{e,1} \ldots \boldsymbol{\omega}_{e,N_e}$ are the selected extreme scenarios extracted from the historical records. The approach is divided into 3 detailed steps. Firstly, the MVEE algorithm is used to find the boundary of the region containing all the historical scenarios. Then, the scaling factor is used to enlarge or shrink the robust region proportionally. Finally, the two-stage robust optimization is adopted to solve the economic dispatch of the distribution system with uncertainty.

A. MVEE algorithm and the initial uncertainty set

A full-dimensional ellipsoid E represented by a symmetric positive definite matrix $Q \in \boldsymbol{R}^{n\times n}$ and a central vertex $\boldsymbol{c} = [c_1, \ldots, c_n]^T$ can be mathematically defined as:

$$E(Q,\boldsymbol{c}) = \{\boldsymbol{\omega} \in \boldsymbol{R}^n \mid (\boldsymbol{\omega}-\boldsymbol{c})^T Q(\boldsymbol{\omega}-\boldsymbol{c}) \leq 1\} \tag{32}$$

In this work, the volume of the feasible region is used to quantify its "size." Because the ellipsoid can be linearly transformed from a sphere in $\boldsymbol{R}^n$ space, the volume of E can be calculated by the volume of the unit sphere ρ_n times the transformation:

$$Vol(E) = \rho_n \det Q^{-\frac{1}{2}} \tag{33}$$

To obtain the ellipsoid with minimum volume following optimization, problem (34) is formulated to determine Q and $\boldsymbol{c}$

$$\begin{aligned} &\min \rho_n \det Q^{-\frac{1}{2}} \\ &s.t. \quad (\boldsymbol{\omega}_{h,1}-\boldsymbol{c})^T Q(\boldsymbol{\omega}_{h,1}-\boldsymbol{c}) \leq 1 \\ &\qquad (\boldsymbol{\omega}_{h,2}-\boldsymbol{c})^T Q(\boldsymbol{\omega}_{h,2}-\boldsymbol{c}) \leq 1 \\ &\qquad \ldots \end{aligned} \tag{34}$$

where all the historical scenarios $\boldsymbol{\omega}_{h,i}$ are taken into account. The reformulated optimization (34) is convex, so it can be solved with mature algorithms efficiently [33].

Meanwhile, the initial extreme scenarios $\boldsymbol{\omega}_e$ (the vertices of E) can be obtained by transforming the general ellipsoid E into an axial ellipsoid E' using transformations (35):

$$\boldsymbol{\omega}_i' = P \times (\boldsymbol{\omega}_i - \boldsymbol{c}) \tag{35}$$

where $\boldsymbol{\omega}_i$ denotes the scenarios in the original ellipsoid before transformations (35), and $\boldsymbol{\omega}_i'$ denotes the corresponding scenarios in the transformed axial ellipsoid. Transformation matrix P denotes an orthogonal matrix used for orthogonal decomposition $Q = P^T D P = P^{-1} D P$, and D is a diagonal matrix consisting of the eigenvalue λ_i of Q.

After the transformation, the initial extreme scenarios $\boldsymbol{\omega}_{e,i}$ can be obtained using $\boldsymbol{\omega}_{e,i}'$, which denotes the vertices of the axial ellipsoid (36). Fig. 2 illustrates the transformation in a 2-dimensional $\boldsymbol{\omega}$ space.

$$E'(D) = \{\boldsymbol{\omega}' \in \boldsymbol{R}^n \mid \boldsymbol{\omega}'^T D\, \boldsymbol{\omega}' \leq 1\} \tag{36}$$

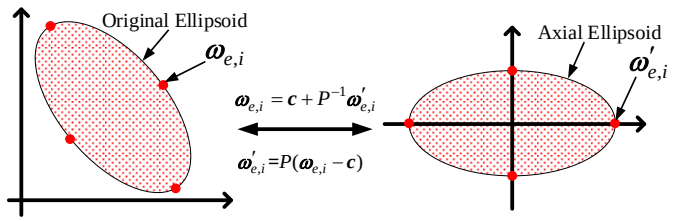

Fig. 2. The relationship between the original ellipsoid and the axial ellipsoid

From the transformation (35) and the axial ellipsoid (36), the extreme scenarios $\boldsymbol{\omega}_{e,i}'$ selected from the axial ellipsoid can be expressed as (37). Finally, the mathematical expression of $\boldsymbol{\omega}_e$ can be obtained combining (37) with (38). The initial uncertainty set can be transformed back using (39)

$$[\boldsymbol{\omega}_{e,1}' \quad \cdots \quad \boldsymbol{\omega}_{e,N_e}'] = \pm diag\left(\frac{1}{\sqrt{\lambda_1}}, \ldots, \frac{1}{\sqrt{\lambda_n}}\right) \tag{37}$$

$$\boldsymbol{\omega}_i = \boldsymbol{c} + P^{-1}\boldsymbol{\omega}_i' \tag{38}$$

$$\boldsymbol{\omega} \in W_{initial} = \left\{ \boldsymbol{\omega} \in \boldsymbol{R}^n \left| \begin{array}{l} \boldsymbol{\omega} = \sum_{i=1}^{N_e} p_i \left(\boldsymbol{c} + P^{-1}\boldsymbol{\omega}_{e,i}'\right) \\ \sum_{i=1}^{N_e} p_i = 1,\ p_i \geq 0 \end{array} \right. \right\} \tag{39}$$

B. The scaling factor

After the initial uncertainty set is obtained, it can be seen that for n-dimensional $\boldsymbol{\omega}$, the number of the extracted extreme scenarios N_e is $2 \times n$. The number of the extreme scenarios is polynomial instead of exponential, with the number of the DRGs, which helps to reduce the computational burden.

However, since the region covered by the convex hull $W_{initial}$ is smaller than the ellipsoid, the initial uncertainty set

This article has been accepted for publication in a future issue of this journal, but has not been fully edited. Content may change prior to final publication. Citation information: DOI 10.1109/TSG.2018.2834952, IEEE Transactions on Smart Grid

may not be able to cover all of the historical scenarios, as shown in Fig.3. Therefore, a scaling factor is adopted here to enlarge the robust region $W_{initial}$. This process is shown in Fig.3 schematically. The scaling factor is determined following the steps below.

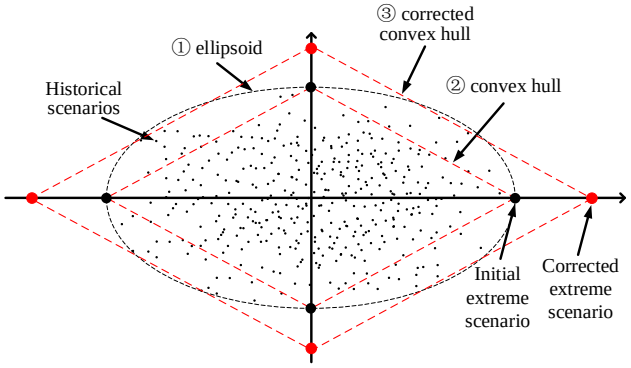

Fig. 3. Lead-out of the scaling factor

First, the historical and the initial extreme scenarios are transformed using (35). The transformation makes the historical scenarios distribute evenly in each quadrant, and the extreme scenarios are located on the coordinate axis.

According to the convex set theory, each historical scenario $\boldsymbol{\omega}'_{h,i}$ in the convex hull can be expressed as linear combinations of the extreme scenarios $\boldsymbol{\omega}'_e$:

$$\begin{aligned} \boldsymbol{\omega}'_{h,i} &= \alpha_{1,i}\boldsymbol{\omega}'_{e,1} + \cdots + \alpha_{N_e,i}\boldsymbol{\omega}'_{e,N_e}, i = 1,\ldots,N_h \\ \alpha_{1,i} + \cdots + \alpha_{N_e,i} &= 1, \alpha_{j,i} \geq 0 \end{aligned} \tag{40}$$

The convex hull should be expanded using the isometric scaling factor k ($k > 1$) if it is to cover the external point. Then (40) should be reformulated as:

$$\begin{aligned} \boldsymbol{\omega}'_{h,i} &= \alpha_{1,i} \times (k_i\boldsymbol{\omega}'_{e,1}) + \cdots + \alpha_{N_e,i} \times (k_i\boldsymbol{\omega}'_{e,N_e}), i = 1,\ldots,N_h \\ \alpha_{1,i} + \cdots + \alpha_{N_e,i} &= 1, \alpha_{j,i} \geq 0 \end{aligned} \tag{41}$$

Furthermore, (41) is equivalent to (42):

$$\begin{aligned} \boldsymbol{\omega}'_{h,i} &= \beta_{1,i}\boldsymbol{\omega}'_{e,1} + \cdots + \beta_{N_e,i}\boldsymbol{\omega}'_{e,N_e}, i = 1,\ldots,N_h \\ \beta_{1,i} + \cdots + \beta_{N_e,i} &= k_i \\ \beta_{j,i} &= k_i\alpha_{j,i} \geq 0 \end{aligned} \tag{42}$$

It is evident that the scaling factor k_i increases as the distance between the historical scenarios and the convex hull grows. k_i measures this distance. As for a historical scenario inside the hull, it can fall exactly on the boundary by shrinking the hull, where $k_i < 1$. Therefore, it is easy to build an optimization to evaluate the positional relationship between the historical scenarios and the convex hull:

$$\min k_i$$
$$s.t \begin{cases} \begin{pmatrix} \boldsymbol{\omega}'_{e,1} & \cdots & \boldsymbol{\omega}'_{e,N_e} \end{pmatrix} \cdot \begin{pmatrix} \beta_{1,i} & \cdots & \beta_{N_e,i} \end{pmatrix}^T = \boldsymbol{\omega}'_{h,i} \\ \beta_{1,i} + \beta_{2,i} + \cdots + \beta_{N_e,i} = k_i, i = 1 \ldots N_h \end{cases} \tag{43}$$

There are N_h optimizations (43) for N_h historical scenarios. The computational burden depends on N_h. However, there is no coupling between the multiple optimizations, so the N_h optimization problems can be combined into one:

$$\min \sum_{i=1}^{N_h} k_i$$
$$s.t \begin{cases} \begin{pmatrix} \boldsymbol{\omega}'_{e,1} \\ \vdots \\ \boldsymbol{\omega}'_{e,N_e} \end{pmatrix}^T \cdot \begin{pmatrix} \beta_{1,1} & \cdots & \beta_{1,N_h} \\ \vdots & \ddots & \vdots \\ \beta_{N_e,1} & \cdots & \beta_{N_e,N_h} \end{pmatrix} = \begin{pmatrix} \boldsymbol{\omega}'_{h,1} \\ \vdots \\ \boldsymbol{\omega}'_{h,N_h} \end{pmatrix}^T \\ \beta_{1,i} + \beta_{2,i} + \cdots + \beta_{N_e,i} = k_i, i = 1,2,\ldots,N_h \end{cases} \tag{44}$$

At last, the maximum value of k_i denoted as k_{max} is the scaling factor we need. The corrected extreme scenarios $\tilde{\omega}_{e,i}$ can be expressed as (45). The corrected uncertainty set can be defined as (46).

$$\tilde{\boldsymbol{\omega}}_{e,i} = \boldsymbol{c} + k_{\max}P^{-1}\boldsymbol{\omega}'_{e,i} = \boldsymbol{c} + k_{\max}\left(\boldsymbol{\omega}_{e,i} - \boldsymbol{c}\right) \tag{45}$$

$$\boldsymbol{\omega} \in W_{cor} = \left\{ \boldsymbol{\omega} \in \boldsymbol{R}^n \middle| \begin{matrix} \boldsymbol{\omega} = \sum_{i=1}^{N_e} p_i\tilde{\boldsymbol{\omega}}_{e,i} \\ \sum_{i=1}^{N_e} p_i = 1,\ p_i \geq 0 \end{matrix} \right\} \tag{46}$$

C. *Two-stage robust optimization*

The optimization model with uncertainty based on the previous section can be generalized in a compact form as (28). The objective function q is linear. f and part of g [(10), (16), (17), (20), (23), (25), denoted as g_1] are linear and the quadratic part of g_2 [(27)] is convex. According to the two-stage strategy proposed in Section II(A), for different scenarios ($\boldsymbol{\omega}_1, \boldsymbol{\omega}_2, \ldots$), there could be different decisions for the second category of variables $\boldsymbol{x}_1, \boldsymbol{x}_2, \ldots$, but the single decision for $\boldsymbol{y}$, and the single decision should be adaptive to all of the selected scenarios. With the two categories of variables, the optimization (28) can be expanded as:

$$\max_{\boldsymbol{\omega}_i \in W_{cor}} \min_{\boldsymbol{x},\boldsymbol{y}} q(\boldsymbol{\omega}, \boldsymbol{x}, \boldsymbol{y})$$
$$s.t \begin{cases} f(\boldsymbol{\omega}_i, \boldsymbol{x}_i, \boldsymbol{y}) = 0,\ g(\boldsymbol{\omega}_i, \boldsymbol{x}_i, \boldsymbol{y}) \leq 0 \\ i = 1, 2\ldots \end{cases} \tag{47}$$

The two-stage decision process is as follows: Firstly, the state of the inflexible facilities is decided using the above optimization (47). Then, the second category of variables is determined by the optimization where the first category of variables $\boldsymbol{y}$ is fixed and the stochastic variables $\boldsymbol{\omega}$ are replaced by selected scenarios. In general, the number of the scenarios in the uncertainty set is infinite and the optimization (47) seems unsolvable. However, the extreme-scenarios are sufficient to deal with optimization (47) and satisfy the robustness actually.

***Theorem* 1**: if the decision variables $\boldsymbol{x}_{e,1}, \ldots, \boldsymbol{x}_{e,N_e}$ and $\boldsymbol{y}$ are adaptive to all the N_e extreme scenarios $\boldsymbol{\omega}_{e,1}, \ldots, \boldsymbol{\omega}_{e,N_e}$, it can ensure the existence of $\boldsymbol{x}_i$ and $\boldsymbol{y}$ in any scenario $\boldsymbol{\omega}_i \in W_{cor}$.

Theorem 1 indicates the equivalency between (47) and following (48).

$$\max_{\boldsymbol{\omega}} \min_{\boldsymbol{x},\boldsymbol{y}} q(\boldsymbol{\omega}, \boldsymbol{x}, \boldsymbol{y})$$
$$s.t \begin{cases} f(\boldsymbol{\omega}_{e,i}, \boldsymbol{x}_{e,i}, \boldsymbol{y}) = 0,\ g(\boldsymbol{\omega}_{e,i}, \boldsymbol{x}_{e,i}, \boldsymbol{y}) \leq 0 \\ i = 1, 2\ldots N_e \end{cases} \tag{48}$$

Proof: For the model suggested in this paper, f and g_1 are linear functions.

$$\begin{cases} f(\boldsymbol{\omega}, \boldsymbol{x}, \boldsymbol{y}) = A_1\boldsymbol{\omega} + B_1\boldsymbol{x} + C_1\boldsymbol{y} = 0 \\ g_1(\boldsymbol{\omega}, \boldsymbol{x}, \boldsymbol{y}) = A_2\boldsymbol{\omega} + B_2\boldsymbol{x} + C_2\boldsymbol{y} \le 0 \end{cases} \tag{49}$$

In addition, the quadratic inequality g_2 is a convex function with second-stage variables $\boldsymbol{x}$ only. Assume $\boldsymbol{x}$ has $N+1$ dimensions, its generalized form can be written as:

$$g_2(\boldsymbol{x}) = \sqrt{\sum_{i=1}^{N} x_i^2} - x_{N+1} \le 0 \tag{50}$$

Since $\boldsymbol{\omega}_i \in W_{cor}$, there exists a set of positive real numbers $p_1, \ldots, p_{N_e}$, satisfying $\sum_{j=1}^{N_e} p_j = 1$ and $\boldsymbol{\omega}_i = \sum_{j=1}^{N_e} p_j \times \boldsymbol{\omega}_{e,j}$. Apply these positive real numbers to the constraints in f and g:

$$\begin{cases} p_i g(\boldsymbol{\omega}_{e,i}, \boldsymbol{x}_{e,i}, \boldsymbol{y}) \le 0 \\ p_i f(\boldsymbol{\omega}_{e,i}, \boldsymbol{x}_{e,i}, \boldsymbol{y}) = 0 \\ i = 1, 2 \ldots N_e \end{cases} \tag{51}$$

Summarizing f and g_1, the following (52) can be obtained.

$$\begin{aligned} &\sum_{j=1}^{N_e} p_j g_1(\boldsymbol{\omega}_{e,j}, \boldsymbol{x}_{e,j}, \boldsymbol{y}) = g_1\left(\sum_{j=1}^{N_e} p_j \boldsymbol{\omega}_{e,j}, \sum_{j=1}^{N_e} p_j \boldsymbol{x}_{e,j}, \boldsymbol{y}\right) \\ &\sum_{j=1}^{N_e} p_j f(\boldsymbol{\omega}_{e,j}, \boldsymbol{x}_{e,j}, \boldsymbol{y}) = f\left(\sum_{j=1}^{N_e} p_j \boldsymbol{\omega}_{e,j}, \sum_{j=1}^{N_e} p_j \boldsymbol{x}_{e,j}, \boldsymbol{y}\right) \end{aligned} \tag{52}$$

As for convex function, g_2 (53) can be obtained by using *Jensen*'s inequality.

$$\sum_{j=1}^{N_e} p_j g_2(\boldsymbol{x}_{e,j}) \ge g_2\left(\sum_{j=1}^{N_e} p_j \boldsymbol{x}_{e,j}\right) \tag{53}$$

For the second-stage variables $\boldsymbol{x}$, its feasible region is also a convex set. So, the linear combination $\boldsymbol{x}_{h,i} = \sum_{j=1}^{N_e} p_j \times \boldsymbol{x}_{e,j}$ is also inside the feasible region. This means that the solution $\boldsymbol{x}_i$ and $\boldsymbol{y}$ for the scenario $\boldsymbol{\omega}_i \in W_{cor}$ exists.

Thus, the proof is completed.

According to the robust optimization theory [28], (48) denotes that the objective function of the optimization is based on the worst-case scenario and guarantees the satisfaction of the constraints in all extreme scenarios. To solve the max-min problem effectively, a dummy variable F is introduced in this paper to replace the maximum of q, and (48) can be reformulated as:

$$\min \ F$$
$$s.t \begin{cases} f(\boldsymbol{\omega}_{e,i}, \boldsymbol{x}_{e,i}, \boldsymbol{y}) = 0, \ g(\boldsymbol{\omega}_{e,i}, \boldsymbol{x}_{e,i}, \boldsymbol{y}) \le 0 \\ F = \max_{\boldsymbol{\omega}} q(\boldsymbol{\omega}, \boldsymbol{x}, \boldsymbol{y}) \\ i = 1, 2 \ldots N_e \end{cases} \tag{54}$$

On the other hand, limited scenarios are embedded in (54). Therefore, (54) is equivalent to (55) according to the definition of the worst-case scenario, and the optimization becomes solvable.

$$\min \ F$$
$$s.t \begin{cases} f(\boldsymbol{\omega}_{e,i}, \boldsymbol{x}_{e,i}, \boldsymbol{y}) = 0, \ g(\boldsymbol{\omega}_{e,i}, \boldsymbol{x}_{e,i}, \boldsymbol{y}) \le 0 \\ F \ge q(\boldsymbol{\omega}_{e,i}, \boldsymbol{x}_{e,i}, \boldsymbol{y}) \\ i = 1, 2 \ldots N_e \end{cases} \tag{55}$$

D. Summary of proposed method

The proposed DARO method is summarized as follows:

First, the positive definite matrix Q and the central vertex $\boldsymbol{c}$ are determined by the historical scenarios using optimization (34). Furthermore, the eigenvalues $\lambda_1 \ldots \lambda_n$ of Q are obtained and the initial uncertainty set can be obtained using (39).

Then, the initial uncertainty set is corrected. The historical scenarios and the initial extreme scenarios are transformed using (35) to check the positional relationship between the historical scenarios and initial uncertainty set. The optimization (44) is used to get the scaling factor k_{max} so as to ensure that all the scenarios are covered by the corrected convex hull. The corrected uncertainty set can be obtained through (46).

Finally, the two-stage robust optimization model can be reformulated as (55) and it can be solved easily using commercial solvers.

The major advantage of the proposed method is that it reduces the conservativeness of the decision. Besides, the computational burden is reduced by limited extreme scenarios. The flowchart of the proposed method is shown in Fig.4.

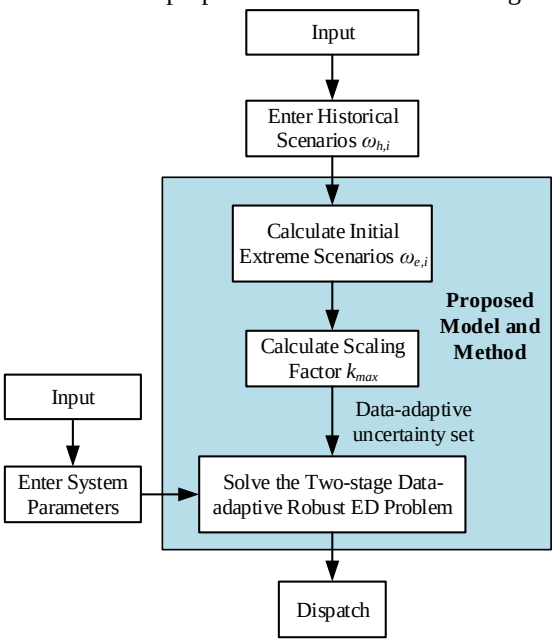

Fig. 4. The flowchart of the proposed model and method

IV. Numerical Results

To validate the effectiveness of the proposed DARO method, two test systems including 33-bus and 123-bus distribution networks are studied. Besides, the IBM ILOG CPLEX is used as the MIQCP solver.

A. System description

For the 33-bus system, the total load is 3.715MW+ 1.86MVar. The topology of the system is shown in Fig. 5. Branch 10-11 and 15-16 are transformers equipped with tap changers, denoted as T1/T2, respectively. The capacity of the switching capacitors installed on the bus 21 and 32 are 0.3MVar and 0.9MVar, respectively. There is also one wind generation site and one photovoltaic (PV) system connected to bus 13 and 17.

This article has been accepted for publication in a future issue of this journal, but has not been fully edited. Content may change prior to final publication. Citation information: DOI 10.1109/TSG.2018.2834952, IEEE Transactions on Smart Grid

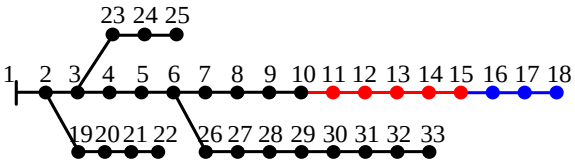

Fig.5. 33-bus system topology

For the 123-bus system, the total load is 5.048MW+ 2.682MVar. Branch 47-49, 87-89, 105-108, and 60-119 are transformers equipped with tap changers, denoted as T1~T4, respectively. The capacity of the switching capacitors installed on the bus 17, 66, and 122 are 1.2MVar, 0.9MVar, and 1.2MVar, respectively. There is also one wind generator installed on bus 51 and 3 photovoltaic systems installed on bus 76, 93, and 102.

The minimum step change of tap ratio is set to 0.025, and the regulation range is set to [0.95, 1.05] for all the transformers. The value of each bank switching capacitor is 0.1MVar. Besides, each switching capacitor installs continuously adjusted SVG, where the capacity is [-0.05MVar, 0.05MVar]. Besides, the one year's output data of the DRGs is obtained from the historical data in a certain region of Australia [46].

B. *Comparative study between DARO and existing TRO*

With given system parameters and historical data, the robust optimization using the cubic set and the data-adaptive set are compared in this section. The data-adaptive set is generated using the method proposed in this paper, while the maximum and the minimum output power of each DRG constitute the cubic set. The comparison of the data-adaptive set and the cubic set is shown in Fig. 6. It can be seen that the data-adaptive set covers a smaller area than the cubic set, which means that when the cubic set is applied to describe the uncertainty, a lot of non-existent scenarios are included. To evaluate the effectiveness of the proposed method, following aspects are compared between the DARO and the existing TRO in [30].

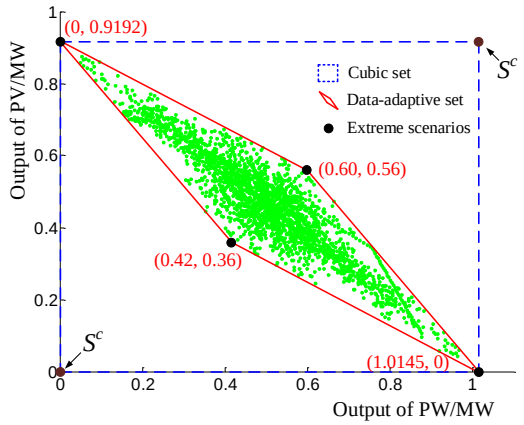

Fig. 6. An illustrative diagram of the data-adaptive set and the cubic set

1) *The robustness of the first-stage variables*

Firstly, the first-stage variables including the switching capacitor and the transformer taps are determined using the DARO method and the TRO method, denoted as y_D and y_T, respectively. The results in the different operation conditions are shown in Table I. When the first-stage is fixed, the historical scenarios are used one by one to check whether the regulation devices such as SVG can provide sufficient flexibility to maintain the balance of active and reactive power. The comparisons are also shown in Fig. 6. The historical operating scenarios with successful second-stage optimality are indicated by the green dots. From Table I and Fig. 6, the DARO with smaller uncertainty set, is as robust as the TRO.

TABLE I. THE FIRST-STAGE VARIABLES IN DIFFERENT OPERATION CONDITIONS FOR 33-BUS SYSTEM

Lower boundary of the voltage	y_D		y_T	
0.8 p.u	T1/T2	C21/C32	T1/T2	C21/C32
	1.025/1	1/7	1.05/1.05	2/7
0.85 p.u	T1/T2	C21/C32	T1/T2	C21/C32
	1.025/1	1/7	1.05/1.05	2/7
0.95 p.u	T1/T2	C21/C32	T1/T2	C21/C32
	1.025/1	2/7	1.025/1	2/9

2) *The conservativeness of the decision*

Over-conservativeness in this work is defined as being robust to the scenarios that rarely happen. It results in two-fold negative impacts.

First, over-conservativeness degrades the economy of the decision. The network losses under the worst-case scenario using DARO and TRO are compared. Besides, 1000 historical scenarios are sampled, and the mean value of the network losses is compared. The results in Table II shows that DARO has the better economy than the TRO either under the worst-case scenario or expectation of all of the historical scenarios.

TABLE II. THE ECONOMY COMPARISON RESULTS IN DIFFERENT OPERATION CONDITIONS FOR 33-BUS SYSTEM

Lower boundary of the voltage	Test scenario	The network loss (MW)	
		Proposed method: DARO	Comparative method: current TRO [30]
0.8 p.u	worst-case scenario	0.14531	0.23648
	historical scenario	0.1287	0.1452
0.85 p.u	worst-case scenario	0.14531	0.23648
	historical scenario	0.1287	0.1452
0.95 p.u	worst-case scenario	0.14531	0.24496
	historical scenario	0.1287	0.1324

On the other hand, over-conservativeness potentially enhances the requirements to the system configuration, e.g., more reactive compensation devices. Table I has already shown that since the uncertainty set obtained by TRO is larger than DARO, more reactive power compensation devices in ADN are turned on. Fig.7 further shows that given the same system configuration, it is more likely for DARO to obtain the robust feasible solution than TRO. Simulation experiments indicate that if we limit the capacity of the reactive power injection from the upper-level grid, there could be no feasible first-stage solution, i.e., failure cases in Fig. 7. For DARO, 0.659MVar at least is needed to maintain the voltage level above 0.95 p.u., while using TRO, 0.751MVar at least is required to maintain the voltage above 0.85, and 0.869MVar at least to keep the voltage above 0.95.

This article has been accepted for publication in a future issue of this journal, but has not been fully edited. Content may change prior to final publication. Citation information: DOI 10.1109/TSG.2018.2834952, IEEE Transactions on Smart Grid

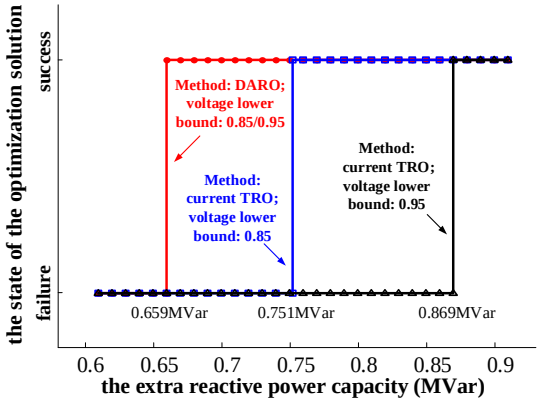

Fig. 7. The status of the optimization solution with the extra reactive power and the voltage bound changing

3) Worst-case scenarios

The worst-case scenarios selected by TRO and DARO are shown in Table III.

TABLE III. THE WORST-CASE SCENARIOS IN DIFFERENT OPERATION CONDITIONS FOR A 33-BUS SYSTEM

Lower bound of the voltage	The output power of DRGs in the worst-case scenario (MW)	
	Proposed method: DARO	Comparative method: current TRO [30]
0.8 p.u	PW=0, PV=0.9192	PW=0, PV=0
0.85 p.u	PW=0, PV=0.9192	PW=0, PV=0
0.95 p.u	PW=0, PV=0.9192	PW=1.0145, PV=0.9192

Together with the long-term historical data shown in Fig. 6, Table III shows that there is a strong correlation between the DRGs in this region. The worst-case scenario considered in the cubic set (denoted as S^c) does not appear in the historical record. From the engineering perspective, we can assume that the probability of scenario S^c and its surrounding area are very small. Therefore, the scenarios like S^c can be ignored in the economic dispatch. From the mathematical point of view, neglecting such correlation leads to blank areas in the robust region where there could be low probability scenarios such as S^c. These scenarios result in over-conservative decisions.

C. Validation of the proposed DARO

The comparison of the conservativeness and the computational efficiency between the DARO and the current TRO in IEEE 123-bus system are shown in Table IV. It can be seen that the operational cost and the reactive compensation of the DARO are less than the TRO as well. In addition, the reactive power compensation device placed on the bus 17, 66, and 122 are enough to balance the reactive power demand when using the DARO. However, with the current TRO, more than 0.221MVar extra reactive power compensation is needed to guarantee the existence of the second-stage optimization. Through this comparison, the economy from the configuration point-of-view can be improved using the DARO. Furthermore, when using the DARO proposed in this paper, much shorter computational time is needed, which verifies the effectiveness of the proposed algorithm.

TABLE IV. DECISION VARIABLES AND CALCULATING TIME FOR 123-BUS SYSTEM

Lower bound of the voltage: 0.85 p.u	Proposed method: DARO		Comparative method: current TRO [30]	
First-stage variables	T1/T2/T3/T4	C17/C66/C122	T1/T2/T3/T4	C17/C66/C122
	1.05/1.05/0.95/1.05	9/8/10	1.05/1.05/0.95/1.05	10/8/12
The worst-case scenario (MW)	PW=0.792, PV1=PV2=PV3=0		PW=PV1=PV2=PV3=0	
Network loss in the worst-case scenario	0.34843 MW		0.46288 MW	
Calculating time	32.4506 s		97.8579 s	

Furthermore, according to the convex relaxation in Section II(A), the equality constraints are transformed to the inequality constraints [30]. To validate the equivalency between the problems before and after transformation, the error index is defined as (56) to see if the equality constraints can be met:

$$\Delta = \left| P_{ij}^2 + Q_{ij}^2 - I_{ij}^2 \cdot U_i^2 \right| \tag{56}$$

From the physical system point of view, small enough Δ indicates that the optimal solution is technically feasible in the power grid. For the non-adjustable variables determined at the first stage optimization, the error for all the extreme scenarios is summed. For the adjustable variables at the second stage, the error for all the possible scenarios is summed. The test results are shown in Table V, from which it can be seen that the equivalency of the power balance constraint is satisfied with negligible error.

TABLE V. THE TESTING OF THE CONIC RELAXATION

Test system	First-stage optimization	Second-stage optimization
33-bus system	6.8824e-06	1.1195e-07
123-bus system	1.7971e-07	2.6564e-06

V. CONCLUSION

In this paper, the data-adaptive robust optimization method for the economic dispatch of ADNs with renewables is proposed. Combining the advances of scenario-generation algorithms and two-stage robust optimization, the proposed DARO method can make full use of the empirical knowledge obtained from the historical data. It is theoretically proved that if the decision is robust to all of the selected extreme scenarios, it is robust to all of the possible scenarios. Case studies show that the proposed algorithm balances the robustness and economics of system operation well by taking the correlations of the DRGs into account. The proposed algorithm is superior to the current two-stage robust optimization with less conservativeness without the loss of security. In addition, the computational efficiency is significantly improved by reducing the number of selected scenarios so that the proposed method is applicable to large distribution systems with lots of DRGs.

REFERENCES

[1] J. Fang, Q. Zeng, X. Ai, Z. Chen, and J. Wen, "Dynamic optimal energy flow in the integrated natural gas and electrical power systems," *IEEE Trans. Sustain. Energy*, vol. 9, no. 1, pp. 188-198, Jun. 2017.

[2] J. Liu, J. Wen, W. Yao, and Y. Long. "Solution to short-term frequency response of wind farms by using energy storage systems," *IET Renewable Power Gener.*, vol. 10, no. 5, pp. 669-678, Apr. 2016.

[3] P. Liu, and Z. Tan, "How to develop distributed generation in China: In the context of the reformation of electric power system," *Renew. Sustain. Energy Rev.*, no. 66, pp. 10–26, Aug. 2016.

[4] Y. Shen, W. Yao, J. Wen, and H. He. "Adaptive wide-area power oscillation damper design for photovoltaic plant considering delay compensation," *IET Gener. Transm. Distrib.*, in press.

[5] W. K. A. Najy, H. H. Zeineldin, and W. L. Woon, "Optimal protection coordination for Microgrids with grid-connected and islanded capability," *IEEE Trans. Ind. Electron.*, vol. 60, no. 4, pp. 1668-1677, Apr. 2013.

[6] Y. Wang, N. Zhang, C. Kang, M. Miao, R. Shi, and Q. Xia, "An efficient approach to power system uncertainty analysis with high-dimensional dependencies," *IEEE Trans. Power Syst.*, vol. 33, no. 3, pp. 2984–2994, May 2018.

[7] Y. Xu, Z. Yang, W. Gu, M. Li, and Z. Deng, "Robust real-time distributed optimal control based energy management in a smart grid," *IEEE Trans. Smart Grid*, vol. 8, no. 4, pp. 1568-1579, Jul. 2017.

[8] C. Lin, W. Wu, X. Chen, and W. Zheng, "Decentralized dynamic economic dispatch for integrated transmission and active distribution networks using multi-parametric programming," *IEEE Trans. Smart Grid*, in press.

[9] J. Li, J. Fang, J. Wen, Y. Pan, and Q. Ding, "Optimal trade-off between regulation and wind curtailment in the economic dispatch problem," *CSEE J. Power Energy Syst.*, vol. 1, no. 4, pp. 37-45, Dec. 2015.

[10] K. Chen, W. Wu, B. Zhang, and H. Sun, "Robust restoration decision-making model for distribution networks based on information gap decision theory," *IEEE Trans. Smart Grid*, vol. 6, no. 2, pp. 587–597, Mar. 2015.

[11] L. Yang, M. He, V. Vittal, and J. Zhang, "Stochastic optimization-based economic dispatch and interruptible load management with increased wind penetration," *IEEE Trans. Smart Grid*, vol. 7, no. 2, pp. 730-739, Mar. 2016.

[12] X. Ai, J. Wen, T. Wu, and W. J. Lee, "A discrete point estimate method for probabilistic load flow based on the measured data of wind power," *IEEE Trans. Ind. Appl.*, vol. 49, no. 5, pp. 2244-2252, Sep. 2013.

[13] Y. Wang, N. Zhang, Q. Chen, J. Yang, C. Kang, and J. Huang, "Dependent discrete convolution based probabilistic load flow for the active distribution system," *IEEE Trans. Sustain. Energy*, vol. 8, no. 3, pp. 1000-1009, Jul. 2017.

[14] X. Ma, Y. Sun, and H. Fang, "Scenario generation of wind power based on statistical uncertainty and variability," *IEEE Trans. Sustain. Energy*, vol. 4, no. 4, pp. 894-904, Oct. 2013.

[15] A. Papavasiliou, S. S. Oren and R. P. O' Neill, "Reserve requirements for wind power integration: a scenario-based stochastic programming framework," *IEEE Trans. Power Syst.*, vol. 26, no. 4, pp. 2197-2206, Nov. 2011.

[16] H. Gangammanavar, S. Sen and V. M. Zavala, "Stochastic Optimization of Sub-Hourly Economic Dispatch With Wind Energy," *IEEE Trans. Power Syst.*, vol. 31, no. 2, pp. 949-959, Mar. 2016.

[17] D. Lee, and R. Baldick, "Load and wind power scenario generation through the generalized dynamic factor model," *IEEE Trans. Power Syst.*, vol. 32, no. 1, pp. 400-410, Jan. 2017.

[18] M. Cui, D. Ke, Y. Sun, D. Gan, J. Zhang, and B. M. Hodge, "Wind power ramp event forecasting using a stochastic scenario generation method," *IEEE Trans. Sustain. Energy*, vol. 6, no. 2, pp. 422-433, Apr. 2015.

[19] Q. Wang, Y. Guan, and J. Wang, "A chance-constrained two-stage stochastic program for unit commitment with uncertain wind power output," *IEEE Trans. Power Syst.*, vol. 27, no. 1, pp. 206–215, Feb. 2012.

[20] A. Kargarian, Y. Fu, and H. Wu, "Chance-constrained system of systems based operation of power systems," *IEEE Trans. Power Syst.*, vol. 31, no. 5, pp. 3404–3413, Sep. 2016.

[21] Y. Cao, Y. Tan, C. Li, and C. Rehtanz, "Chance-constrained optimization-based unbalanced optimal power flow for radial distribution networks," *IEEE Trans. Power Del.*, vol. 28, no. 3, pp. 1855-1864, Jul. 2013.

[22] R. Jiang, J. Wang, and Y. Guan, "Robust unit commitment with wind power and pumped storage hydro," *IEEE Trans. Power Syst.*, vol. 27, no. 2, pp. 800-810, May. 2012.

[23] R. Jiang, J. Wang, M. Zhang, and Y. Guan, "Two-stage minimax regret robust unit commitment," *IEEE Trans. Power Syst.*, vol. 28, no. 3, pp. 2271–2282, Aug. 2013.

[24] A. Soroudi, P. Siano, and A. Keane, "Optimal DR and ESS scheduling for distribution losses payments minimization under electricity price uncertainty," *IEEE Trans. Smart Grid*, vol. 7, no. 1, pp. 261-272, Jan. 2016.

[25] C. Peng, P. Xie, L. Pan, and R. Yu, "Flexible robust optimization dispatch for hybrid wind/photovoltaic/hydro/thermal power system," *IEEE Trans. Smart Grid*, vol. 7, no. 2, pp. 751-762, Mar. 2016.

[26] G. Liu, Y. Xu, and K. Tomsovic, "Bidding strategy for microgrid in day-ahead market based on hybrid stochastic/robust optimization," *IEEE Trans. Smart Grid*, vol. 7, no. 1, pp. 227-237, Jan. 2016.

[27] Y. Guan, and J. Wang, "Uncertainty sets for robust unit commitment," *IEEE Trans. Power Syst.*, vol. 29, no. 3, pp. 1439–1440, May. 2014.

[28] R. A. Jabr, "Robust transmission network expansion planning with uncertain renewable generation and loads," *IEEE Trans. Power Syst.*, vol. 28, no. 4, pp. 4558–4567, Nov. 2013.

[29] W. Yuan, J. Wang, F. Qiu, C. Chen, and C. Kang, "Robust optimization-based resilient distribution network planning against natural disasters," *IEEE Trans. Smart Grid*, vol. 7, no. 6, pp. 2817-2826, Nov. 2016.

[30] T. Ding, S. Liu, W. Yuan, Z. Bie, and B. Zeng, "A two-stage robust reactive power optimization considering uncertain wind power integration in active distribution networks," *IEEE Trans. Sustain. Energy*, vol. 7, no. 1, pp. 301–311, Jan. 2016.

[31] T. Ding, C. Li, Y. Yang, J. Jiang, Z. Bie, and F. Blaabjerg, "A two-stage robust optimization for centralized-optimal dispatch of photovoltaic inverters in active distribution networks," *IEEE Trans. Sustain. Energy*, vol. 8, no. 2, pp. 744–754, Apr. 2017.

[32] J. Li, J. Wen, and X. Han, "Low-carbon unit commitment with intensive wind power generation and carbon capture power plant," *J. Mod Power Syst. Clean Energy*, vol. 3, no. 1, pp. 63–71, 2015.

[33] T. Ding, J. Lv, R. Bo, Z. Bie, and F. Li, "Lift-and-project MVEE based convex hull for robust SCED with wind power integration using historical data-driven modeling approach," *Renew. Energy*, no. 92, pp. 415–427, Feb. 2016.

[34] M. Farivar, and S. H. Low, "Branch flow model: Relaxations and convexification—Part I," *IEEE Trans. Power Syst.*, vol. 28, no. 3, pp. 2554–2564, Aug. 2013.

[35] S. H. Low, "Convex relaxation of optimal power flow—Part I: formulations and equivalence," *IEEE Trans. Control Netw. Syst.*, pp. 15–27, Aug. 2013.

[36] J. A. Momh, M. E. EI-Hawary, and R. Adapa, "A review of selected optimal power flow literature to 1993. Part I: Nonlinear and quadratic programming approaches," *IEEE Trans. Power Syst.*, vol. 14, no. 1, pp. 96–104, Feb. 1999.

[37] J. A. Momh, M. E. EI-Hawary, and R. Adapa, "A review of selected optimal power flow literature to 1993. Part II: Newton, linear programming and interior point methods," *IEEE Trans. Power Syst.*, vol. 14, no. 1, pp. 105–111, Feb. 1999.

[38] D. Bertsimas, V. Gupta, and N. Kallus, "Data-driven robust optimization," *Mathematics*, Aug. 2013.

[39] S. Liao, W. Yao, X. Han, J. Wen, and S. Cheng. "Chronological operation simulation framework for regional power system under high penetration of renewable energy using meteorological data," *Appl. Energy*, vol. 203, pp. 816-828, Oct. 2017.

[40] X. Xu, X. He, Q. Ai, and R. C. Qiu, "A correlation analysis method for power systems based on random matrix theory," *IEEE Trans. Smart Grid*, vol. 8, no. 4, pp. 1811-1820, Jul. 2017.

[41] W. Yang, R. Negi, C. Faloutsos, and M. D. Ili, "Robust data-driven state estimation for smart grid," *IEEE Trans. Smart Grid*, vol. 8, no. 4, pp. 1956-1967, Jul. 2017.

[42] K. Zhou, C. Fu, and S. Yang, "Big data driven smart energy management: From big data to big insights," *Renew. Sustain. Energy Rev.*, vol. 56, pp. 215-225, 2016.

[43] J. Zou, Q. Chang, J. Arinez, and G. Xiao, "Data-driven modeling and real-time distributed control for energy efficient manufacturing systems," *Energy*, vol. 127, pp. 247-257, 2017.

[44] P. Kumar, and E. A. Yildirim, "Minimum-volume enclosing ellipsoids and core sets," *Journal of Optimization Theory and Applications*, vol. 126, no. 1, pp. 1–21, Jul. 2005.

[45] W. Wu, Z. Tian, and B. Zhang, "An exact linearization method for OLTC of transformer in branch flow model," *IEEE Trans. Power Syst.*, vol. 32, no. 3, pp. 2475–2476, May. 2017.

[46] http://solar.uq.edu.au/user/reportPower.php

Yipu Zhang (**S'18**) received B.S. degree in electrical engineering from Huazhong University of Science and Technology (HUST), China in 2016. Since September 2016, he has been pursuing the M.S. degree in the School of Electrical and Electronics Engineering, HUST, Wuhan, China. His current research interests include robust optimization and renewable energy integration.

Xiaomeng Ai (**S'11-M'17**) obtained the B.Eng degree in mathematics and applied mathematics and Ph.D. in electrical engineering in 2008 and 2014, respectively, both from Huazhong University of Science and Technology (HUST), Wuhan, China. Currently he is a lecturer at HUST. His research interests include robust optimization, stochastic optimization, renewable energy integration and integrated energy market.

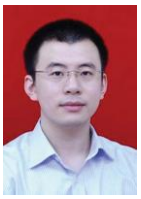

Jiakun Fang (**S'10-M'13**) received the B.Sc. and Ph.D. degrees from Huazhong University of Science and Technology (HUST), China, in 2007 and 2012, respectively.

He is currently an Assistant Professor with the Department of Energy Technology, Aalborg University, Aalborg, Denmark. His research interests include power system dynamic stability control, power grid complexity analysis and integrated energy system.

Jinyu Wen (**M'10**) received the B.S. and Ph.D. degrees in electrical engineering from Huazhong University of Science and Technology (HUST), Wuhan, China, in 1992 and 1998, respectively.

He was a Visiting Student from 1996 to 1997 and Research Fellow from 2002 to 2003 all at the University of Liverpool, Liverpool, UK, and a Senior Visiting Researcher at the University of Texas at Arlington, Arlington, USA, in 2010. From 1998 to 2002 he was a Director Engineer with XJ Electric Co. Ltd. in China. In 2003, he joined the HUST and now is a Professor with the School of Electrical and Electronics Engineering, HUST. His current research interests include renewable energy integration, energy storage, multi-terminal HVDC and power system operation and control.

Haibo He (**F'17**) received the B.S. and M.S. degrees in electrical engineering from Huazhong University of Science and Technology, China, in 1999 and 2002, respectively, and the Ph.D. degree in electrical engineering from Ohio University in 2006. From 2006 to 2009, he was an Assistant Professor at the Department of Electrical and Computer Engineering at Stevens Institute of Technology. Currently, he is the Robert Haas Endowed Chair Professor at the Department of Electrical, Computer, and Biomedical Engineering at the University of Rhode Island. His research interests include adaptive dynamic programming, computational intelligence, machine learning and data mining, and various applications. He has published 1 sole-author research book (Wiley), edited 1 book (Wiley-IEEE) and 6 conference proceedings (Springer), and authored and co-authored over 250 peer-reviewed journal and conference papers. He severed as the General Chair of the IEEE Symposium Series on Computational Intelligence (SSCI 2014). He was a recipient of the IEEE International Conference on Communications Best Paper Award (2014), IEEE Computational Intelligence Society (CIS) Outstanding Early Career Award (2014), National Science Foundation (NSF) CAREER Award (2011), and Providence Business News (PBN) Rising Star Innovator Award (2011). Currently, he is the Editor-in-Chief of the IEEE Transactions on Neural Networks and Learning Systems.